A Cube-Based Scheme of IE-ODDM-MLFMA for Electromagnetic Scattering Problems

Wei-Dong Li, Hou-Xing Zhou, and Wei Hong, *Senior Member, IEEE*

***Abstract*—A cube-based scheme of integral-equation-based overlapped domain decomposition method with multilevel fast multipole algorithm (IE-ODDM-MLFMA) is proposed for the analysis of electromagnetic (EM) scattering problems. In this scheme, each bottom cube is located either inside an iterative region or inside the corresponding incident region, and the iterative and incident regions are complementary to each other from the bottom cube point of view, which makes it convenient to implement the ODDM in the frame of the MLFMA. Numerical examples are presented to validate the proposed scheme.**

***Index Terms*—Electromagnetic (EM) scattering, multilevel fast multipole algorithm (MLFMA), overlapped domain decomposition method (ODDM).**

I. Introduction

THE method of moments (MoM) [1] with RWG functions [2] is widely used for formulating 3D electromagnetic (EM) scattering problems. It needs $O(N^2)$ memory to store the matrix and $O(N^2)$ operations to perform the matrix vector product via an iterative solver. The fast multipole method (FMM) [3] and its multilevel version, multilevel fast multipole algorithm (MLFMA) [4], lower them to $O(N^{1.5})$ and $O(N \log N)$, respectively. However, the MLFMA still suffers from the consumption of CPU time and storage when solving very large problems.

Based on the integral-equation-based overlapped domain decomposition method (IE-ODDM) [5] and the MLFMA, an IE-ODDM-MLFMA scheme was developed in the authors' previous work [6] to further enhance the efficiency of the MLFMA and to make larger problems solvable. In this scheme, the outer iteration is very fast-convergent due to the spurious edge effect of the current in each subdomain being effectively depressed, and the dominant memory requirement for plane-wave expansions in the MLFMA is significantly reduced. However, when the aggregation and disaggregation for a pair of iterative and incident regions are implemented, RWG elements in the bottom cubes are always identified by the attribute of being located inside the iterative or incident region. Additionally, cumbersome details [6] are needed to implement the near-part matrix vector product and to construct the preconditioner for the iterative region. This is caused by the dual roles of the bottom cubes located inside a pair of iterative and incident regions, i.e., both the leaves of the oct-tree for the iterative region and those of the oct-tree for the corresponding incident region.

In this letter, a modification is made for the buffer region in the bottom cubes located both inside the iterative region and inside the corresponding incident region, which generates a new pair of iterative and incident regions. Each new iterative region is complementary to the corresponding incident region from the bottom cube point of view. Based on the new iterative and incident regions, a novel IE-ODDM-MLFMA scheme is constructed with a little modification in the frame of the MLFMA, which greatly simplified the implementation of the IE-ODDM-MLFMA.

II. Cube-Based Scheme of IE-ODDM-MLFMA

An arbitrarily shaped perfectly electric conducting (PEC) object illuminated by plane waves is considered. Because the ODDM combined with the MoM and the MLFMA was detailed respectively in [5] and [6], here we only review the formulas briefly. The ODDM is expressed in matrix form as

$$\tilde{Z}_{ii}\tilde{J}_i^{(k)} = W_i, \quad i = 1, 2, \cdots, M \tag{1}$$

where

$$W_i = \tilde{V}_i - \sum_{j \neq i, c(j) \notin b(i)} \tilde{Z}_{ij}\tilde{I}_j. \tag{2}$$

$\tilde{J}_i^{(k)}$ is the vector of the current coefficients to be solved in the ith iterative region Ω_i during the kth outer iteration; $\tilde{I}_j$ is the vector of the latest solved current coefficients in the jth subdomain during the kth or $(k-1)$th outer iteration. For other notation details, please refer to [5] and [6]. The MLFMA solving (1) is implemented on the basis of the oct-tree for Ω_i; the MLFMA for the matrix vector products in (2) is implemented on the basis of both the oct-tree for Ω_i and the oct-tree for the ith incident region $\overline{\Omega}_i$.

Note that some bottom cubes, located both inside Ω_i and inside $\overline{\Omega}_i$, contain not only RWG elements in Ω_i, but also those in $\overline{\Omega}_i$. Hence, Ω_i is complementary to $\overline{\Omega}_i$ from the RWG element point of view. This also motivates us to call here the IE-ODDM-MLFMA scheme the RWG-based scheme for shortening.

The bottom cubes mentioned play dual roles in the RWG-based scheme, i.e., both leaves of the oct-tree for the iterative region Ω_i and those of the oct-tree for the incident region $\overline{\Omega}_i$.

Manuscript received March 21, 2009. First published May 15, 2009; current version published July 09, 2009. This work was supported by the National Basic Research Program of China (2009CB320203), the Science Fund for Creative Research Groups of China (60621002), the National Hi-Tech Research and Development Program of China (2007AA01Z2B4), and Alfried Krupp Foundation of Germany.

The authors are with the State Key Laboratory of Millimeter Waves, School of Information Science and Engineering, Southeast University, Nanjing 210096, China (e-mail: wdli@emfield.org; hxzhou@emfield.org; weihong@seu.edu.cn).

Digital Object Identifier 10.1109/LAWP.2009.2023096

When dealing with the bottom cubes located both inside Ω_i and inside $\overline{\Omega}_i$ $(i = 1, \cdots, M)$, careful treatments [6] are needed as follows.

1) RWG elements in the above bottom cubes are always identified by the attribute of being located inside Ω_i or $\overline{\Omega}_i$ to perform the aggregation and disaggregation for the corresponding region.
2) When the near-part matrix vector products in (1) and (2) are performed, respectively, the current coefficients corresponding to the RWG elements outside Ω_i and $\overline{\Omega}_i$ are enforced to be zeros, respectively.
3) To construct the preconditioner for Ω_i, some elements are extracted from the block diagonal submatrices in the traditional MLFMA to form some new block diagonal submatrices and the inverses of the new block submatrices are needed.

A new version of the IE-ODDM-MLFMA, here called the cube-based scheme for shortening, will be proposed, in which each bottom cube plays one and only one role—i.e., either a leaf of the oct-tree for the iterative region or a leaf of the oct-tree for the corresponding incident region.

As a simple example, a PEC plate is considered, as shown in Fig. 1. During an outer iteration, the inner subdomain to be solved and the light gray region as its buffer region (as defined in [5] and [6]) compose an iterative region Ω_i, and the other subdomains compose the corresponding incident region $\overline{\Omega}_i$. The bottom cubes, surrounded by the dashed lines, are located both inside Ω_i and inside $\overline{\Omega}_i$ due to containing both the RWG elements (light gray) in Ω_i and the ones (dark gray) in $\overline{\Omega}_i$. The buffer region in each bottom cube is further extended by adding the incident region in the bottom cube, which means that the RWG elements colored by dark gray in the cube are converted into the additional buffer region as shown in Fig. 1. Then, the new buffer region consists of the light and dark gray regions. Consequently, the above bottom cubes and the ones entirely located inside Ω_i compose a new iterative region $\tilde{\Omega}_i$; the remaining bottom cubes are entirely located inside the $\overline{\Omega}_i$, and then compose a new smaller incident region $\tilde{\overline{\Omega}}_i$. In this way, each bottom cube is either a leaf of the oct-tree for the new iterative region or a leaf of the oct-tree for the new incident region. In other words, a new iterative region is complementary to the corresponding new incident region from the bottom cube point view, which is evidently different from the RWG-based scheme and is the basis of the implementation of the cube-based scheme.

In the following, C_{m_L} is an arbitrary bottom cube being located inside $\tilde{\Omega}_i$ $(C_{m_L} \in \tilde{\Omega}_i)$, where L denotes the lowest level of the oct-tree for the entire domain. The cube-based scheme can be formulated through the MLFMA, respectively, in (1) and (2), where Ω_i and $\overline{\Omega}_i$ are replaced with $\tilde{\Omega}_i$ and $\tilde{\overline{\Omega}}_i$ for $i = 1, \cdots, M$, respectively. The electric field integral equation (EFIE) is considered as an example.

The action of the current in $\tilde{\Omega}_i$ on that in $C_{m_L} \in \tilde{\Omega}_i$ for (1) consists of the near and far interactions

$$\sum_{N_{m_L}\in\tilde{\Omega}_i} Z^{near}_{m_L N_{m_L}} X_{N_{m_L}} + \int d^2\hat{k}\, V^{L,f}_{m_L}(\boldsymbol{k})\cdot W_L(\boldsymbol{k},\tilde{\Omega}_i) \quad (3)$$

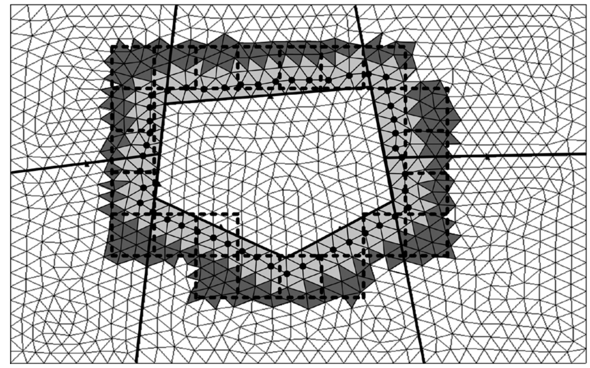

Fig. 1. The new iterative and incident regions. Light gray and dark gray represent the original buffer region and the additional buffer region, respectively, and the dashed lines denote the bottom cubes located both inside the original iterative region and inside the corresponding incident region.

where $X_{N_{m_L}}$ denotes the vector of current coefficients in the neighboring bottom cube N_{m_L} of C_{m_L}, and $\int d^2\hat{k}$ denotes the integral over the unit sphere. The element of the vector $V^{L,f}_{m_L}(\boldsymbol{k})$—i.e., plane-wave expansion for $u \in C_{m_L}$—is

$$V^{L,f}_{um_L}(\boldsymbol{k}) = \int_{S_u} ds(\overline{\overline{I}} - \hat{k}\hat{k})\cdot \boldsymbol{g}_u(\boldsymbol{r}) e^{-j\boldsymbol{k}\cdot(\boldsymbol{r}-\boldsymbol{r}_{m_L})} \quad (4)$$

where $\hat{k} = \boldsymbol{k}/|\boldsymbol{k}|$. When $l_{\text{iter}} \le l \le L$,

$$W_l(\boldsymbol{k},\tilde{\Omega}_i) = e^{-j\boldsymbol{k}\cdot\boldsymbol{r}_{m_l m_{l-1}}} W_{l-1}(\boldsymbol{k},\tilde{\Omega}_i) + \sum_{n_l \notin \{N_{m_l}\}, n_{l-1}\in\{N_{m_{l-1}}\}} \alpha_{m_l n_l}(\boldsymbol{k},\boldsymbol{r}_{m_l n_l}) V^{l,s}_{n_l}(\boldsymbol{k},\tilde{\Omega}_i) \quad (5)$$

where l_{iter} denotes the highest level of the oct-tree for $\tilde{\Omega}_i$ and $\{N_{m_l}\}$ the set of neighboring cubes of C_{m_l}. The incoming wave expansions for C_{m_l} in (5) originate from those for the parent cube $C_{m_{l-1}}$ and the outgoing wave expansions for the unneighboring cube C_{n_l} whose parent cube $C_{n_{l-1}}$ is neighboring to $C_{m_{l-1}}$, where W_{l-1} vanishes when $l = l_{\text{iter}}$. $\alpha_{m_l n_l}(\boldsymbol{k},\boldsymbol{r}_{m_l n_l})$ is the translation operator [4], where $\boldsymbol{r}_{m_l n_l} = \boldsymbol{r}_{m_l} - \boldsymbol{r}_{n_l}$, $\boldsymbol{r}_{m_l}$ and $\boldsymbol{r}_{n_l}$ are the centers of C_{m_l} and C_{n_l}, respectively. The outgoing wave expansion for C_{n_l} is

$$V^{l,s}_{n_l}(\boldsymbol{k},\tilde{\Omega}_i) = \sum_{C_{n_{l+1}}} e^{-j\boldsymbol{k}\cdot\boldsymbol{r}_{n_l n_{l+1}}} \cdots \sum_{C_{n_L}} e^{-j\boldsymbol{k}\cdot\boldsymbol{r}_{n_{L-1} n_L}} \cdot \sum_{v\in C_{n_L}, C_{n_L}\in\tilde{\Omega}_i\setminus\{N_{m_L}\}} \int_{S_v} ds'(\overline{\overline{I}} - \hat{k}\hat{k})\cdot \boldsymbol{g}_v(\boldsymbol{r}') e^{-j\boldsymbol{k}\cdot(\boldsymbol{r}_{n_L}-\boldsymbol{r}')} x_v \quad (6)$$

where x_v is the current coefficient of the RWG function $\boldsymbol{g}_v$.

The action of the current in $\tilde{\overline{\Omega}}_i$ on that in $C_{m_L} \in \tilde{\Omega}_i$ for (2) is written as

$$\sum_{N_{m_L}\in\tilde{\overline{\Omega}}_i} Z^{near}_{m_L N_{m_L}} X_{N_{m_L}} + \int d^2\hat{k}\, V^{L,f}_{m_L}(\boldsymbol{k})\cdot W_L(\boldsymbol{k},\tilde{\overline{\Omega}}_i) \quad (7)$$

where $W_l(\boldsymbol{k},\tilde{\overline{\Omega}}_i)$ and $V^{l,s}_{n_l}(\boldsymbol{k},\tilde{\overline{\Omega}}_i)$ $(l_{\text{inc}} \le l \le L)$ employed in $W_l(\boldsymbol{k},\tilde{\overline{\Omega}}_i)$ are obtained by replacing $\tilde{\Omega}_i$ with $\tilde{\overline{\Omega}}_i$ in (5) and (6), respectively. l_{inc} denotes the highest level of the oct-tree for $\tilde{\overline{\Omega}}_i$.

TABLE I

NUMBERS OF THE INNER ITERATIONS (INSIDE AND OUTSIDE BRACKETS, RESPECTIVELY, FOR THE RWG-BASED SCHEME AND THE CUBE-BASED SCHEME), RELATIVE RESIDUAL ERRORS OF THE OUTER ITERATIONS, AND CPU TIME (MINUTES) FOR THE CUBE-BASED SCHEME AND THE RWG-BASED SCHEME FOR A PEC SPHERE

Outer iteration		1	2	3	4	5
Inner iteration	Region 1	2(3)	4(4)	4(4)	1(1)	1(1)
	Region 2	3(3)	2(2)	3(5)	3(1)	1(1)
	Region 3	3(3)	5(3)	3(3)	1(2)	1(1)
	Region 4	3(3)	3(4)	5(3)	1(1)	1(1)
error(V , k)	Cube-based	0.1389	6.533E-3	7.378E-4	5.330E-4	2.962E-4
	RWG-based	0.1351	7.740E-3	6.296E-4	2.403E-4	2.109E-4
error(I , k)	Cube-based		0.1175	7.600E-3	8.085E-4	5.266E-4
	RWG-based		0.1054	8.236E-3	5.528E-4	3.669E-4
CPU time for outer iteration	Cube-based	9.70	14.00	14.75	7.55	5.95
	RWG-based	10.52	12.78	14.38	6.47	5.75

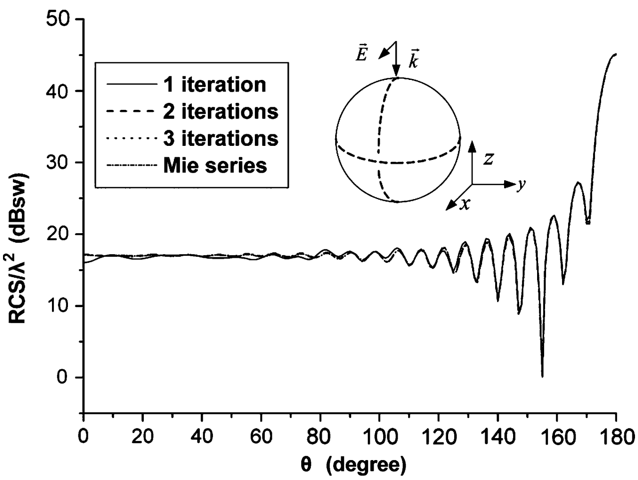

Fig. 2. RCS results for a PEC sphere obtained from the Mie series and the cube-based scheme, respectively. θ is measured from the z-axis in the x-z plane.

It is observed from (3) and (7) that the near-part matrix vectors can be multiplied directly. The formulas (6) and (4) indicate that the aggregation and the disaggregation can be performed without involving such cumbersome details as in the RWG-based scheme. Hence, the cube-based scheme is more conveniently implemented than the RWG-based scheme in the frame of the MLFMA.

Because the iterative region becomes larger and the incident region smaller, the leaves of the oct-tree for the iterative region increase and the nodes of the tree remain unchanged; the leaves of the oct-tree for the incident region lessen, and the nodes of the tree may decrease. Hence, the memory requirement in (1) increases, and that in (2) may decrease. However, we are concerned about whether the cube-based scheme loses its solution accuracy compared with the RWG-based scheme, which will be answered in Section III.

III. NUMERICAL EXAMPLES

In this section, we consider EM scattering problems from a PEC sphere and a PEC cylinder, respectively, to validate the cube-based scheme. In all considered cases, the incident wave is an x-polarized plane wave propagating along the $-z$-axis. The simulations are performed on a personal computer with 3.0-GHz CPU and 2.0-GB RAM. The block-diagonal, incomplete lower and upper triangular matrices (DILU) preconditioner [6] is used to speed up the iterative solution of the cube-based scheme, the RWG-based scheme, and the traditional MLFMA, respectively. The near-part matrices in the three schemes are stored by using the approach in [7], and their memory requirements are not taken into consideration in comparison.

A PEC sphere of radius 4λ is first considered, as shown in Fig. 2. Its surface is averagely split into four subdomains by the dashed line, where 74 304 unknowns are involved. In the MLFMA, 106.28 MB and 54.21 min are used to reach the relative error of 0.001. Fig. 2 compares the radar cross-section (RCS) results obtained from the Mie series [8] and the cube-based scheme, respectively, and shows that the RCS result after three outer iterations from the cube-based scheme agrees well with the analytical solution. The results from one to three outer iterations show that the cube-based scheme is fast convergent.

Table I lists the numbers of the inner iterations, relative errors of the outer iterations, and CPU time for each outer iteration of the cube-based scheme and the RWG-based scheme. $error(V,k)$ and $error(I,k)$ (see [6, eq. (15) and (16)]) for the cube-based scheme are the same order of magnitude as those for the RWG-based scheme, respectively, and they decrease evidently as the outer iteration increases. CPU time for the cube-based scheme after two and three outer iterations is 23.7 and 38.45 min, respectively, and hence, the time is reduced by 56.28% and 29.07%, respectively, compared to the MLFMA. As seen from Table I, the time for the cube-based scheme is slightly more than that for the RWG-based scheme. This is because the iterative region of the former is slightly larger than that of the latter, and thus the solution time grows. The memory requirements of the cube-based scheme and the RWG-based scheme are 51.62 and 52.48 MB, respectively, which means that the storages are reduced by 51.43% and 50.62%, respectively, compared to the MLFMA. The reason for the different storages between the two schemes can be found in Table II, in which the bottom cubes located inside each incident region for the cube-based scheme are 110 fewer than those for the RWG-based scheme.

The next example is a PEC cylinder with its radius 7.5λ and height 10λ, as shown in Fig. 3. The surface is split into four subdomains by the dashed lines, where 285 180 unknowns are involved. In the MLFMA, 366.76 MB and 234.81 min are used to reach the relative error of 0.001. Fig. 3 shows that the cube-

TABLE II
NUMBERS OF THE CUBES LOCATED INSIDE EACH INCIDENT REGION AT DIFFERENT LEVELS FOR THE CUBE-BASED SCHEME AND THE RWG-BASED SCHEME

Level		2	3	4	5
Region 1	Cube-based	42	159	603	2257
	RWG-based	42	159	603	2367
Region 2	Cube-based	42	160	605	2255
	RWG-based	42	160	605	2365
Region 3	Cube-based	42	160	605	2255
	RWG-based	42	160	605	2365
Region 4	Cube-based	42	160	605	2255
	RWG-based	42	160	605	2365

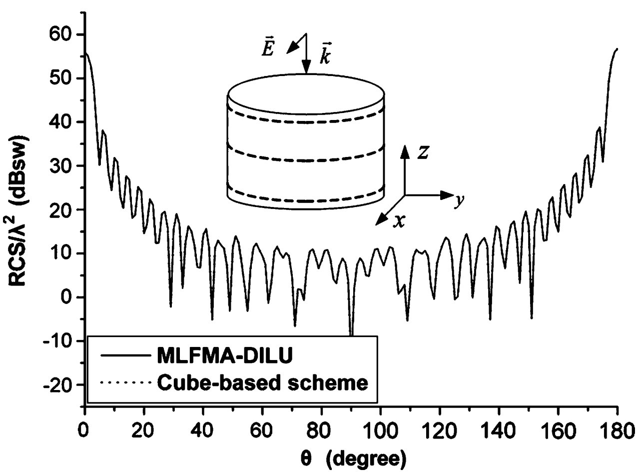

Fig. 3. RCS results for a PEC cylinder obtained from the cube-based scheme and the MLFMA. θ is measured from the z-axis in the x-z plane.

based scheme after three outer iterations gives nearly the same result as the MLFMA. RCS results in Fig. 4 show that the cube-based scheme has a good convergence behavior.

CPU time for the cube-based scheme after two and three outer iterations is 98.36 and 154.24 min, respectively, and hence, the time is reduced by 58.11% and 34.31%, respectively, compared to the MLFMA. The memory requirements of the cube-based scheme and the RWG-based scheme are 165.72 and 169.13 MB, respectively, and then the storages are reduced by 54.82% and 53.89%, respectively, compared to the MLFMA. The cube-based scheme requires slightly less storage than the RWG-based scheme due to the fewer cubes in each incident region at levels 4, 5, and 6.

IV. CONCLUSION

In this letter, a cube-based scheme is proposed for simplifying the implementation of the IE-ODDM-MLFMA for the analysis

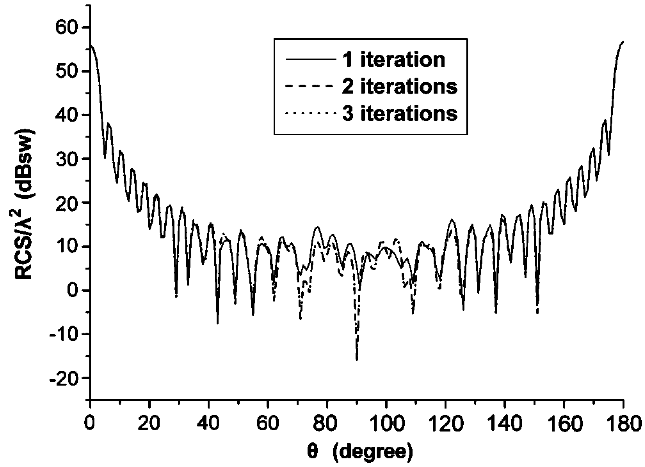

Fig. 4. RCS results convergence for a PEC cylinder.

of electromagnetic scattering problems. Each iterative region in this scheme is complementary to the corresponding incident region from the bottom cube point of view. Numerical examples have demonstrated the validity and efficiency of the cube-based scheme in dealing with some EM scattering problems.

ACKNOWLEDGMENT

The authors would like to thank Prof. T. Weiland of the TEMF Institute in Technische Universität Darmstadt, Germany, for useful comments.

REFERENCES

[1] R. F. Harrington, *Field Computation by Moment Methods*. New York: IEEE Press, 1993.
[2] S. M. Rao, D. R. Wilton, and A. W. Glisson, "Electromagnetic scattering by surfaces of arbitrary shape," *IEEE Trans. Antennas Propag.*, vol. AP-30, no. 3, pp. 409–418, May 1982.
[3] R. Coifman, V. Rokhlin, and S. M. Wandzura, "The fast multipole method for the wave equation: A pedestrian prescription," *IEEE Antennas Propag. Mag.*, vol. 35, no. 3, pp. 7–12, Jun. 1993.
[4] W. C. Chew, J. M. Jin, E. Michielssen, and J. M. Song, *Fast and Efficient Algorithms in Computational Electromagnetics*. Boston, MA: Artech House, 2001.
[5] W.-D. Li, W. Hong, and H.-X. Zhou, "Integral equation-based overlapped domain decomposition method for the analysis of electromagnetic scattering of 3D conducting objects," *Microw. Opt. Tech. Lett.*, vol. 49, no. 2, pp. 265–274, Feb. 2007.
[6] W.-D. Li, W. Hong, and H.-X. Zhou, "An IE-ODDM-MLFMA scheme with DILU preconditioner for analysis of electromagnetic scattering from large complex objects," *IEEE Trans. Antennas Propag.*, vol. 56, no. 5, pp. 1368–1380, May 2008.
[7] P. Havé, "A parallel implementation of the fast multipole method for Maxwell's equations," *Int. J. Numer. Meth. Fluid.*, vol. 43, pp. 839–864, 2003.
[8] J. J. Bowman, T. B. A. Senior, and P. L. E. Uslenghi, *Electromagnetic Scattering by Simple Shapes, Revised*. New York: Hemisphere, 1987.